An Electron Paramagnetic Resonance Study of Mn^{2+} Ions Doped in Langbeinites

T. Böttjer, G. Lehmann[a], and M. Stockhausen

Institut für Physikalische Chemie der Universität Münster, Münster (Germany)

Z. Naturforsch. **47a**, 849–856 (1992); received April 27, 1992

The cubic (high temperature) phase of some langbeinites, $A_2^+B_2^{2+}(SO_4)_3$ with 11 different combinations of A and B type cations, doped with Mn^{2+}, is investigated by EPR. Powder or single crystal spectra are measured at X-band. They indicate centers of axial symmetry in all cases. In 6 of the langbeinites two centers are found which differ considerably in intensity. Both centers are substitutional defects (Mn in the crystallographically nonequivalent divalent B ion sites). For the more intense one the zero field splitting parameter B_2^0 is proved to be negative in all cases. That center is assigned to the more spacious site which, depending on the cation size, allows for local relaxation. It is shown by comparison with predictions of the superposition model that relaxation appears to be effective.

Introduction

Langbeinite, $K_2Mg_2(SO_4)_3$, is a mineral which crystallizes in the cubic space group $P2_13$, the unit cell containing four formula units. The structure is well known [1]. The $Mg_2(SO_4)_3^{2-}$ groups provide cavities for the K cations, which are irregularly coordinated by 9 oxygens. The Mg cations, on the other hand, are coordinated by 6 oxygens in distorted octahedral arrangement. The two kinds of cations appear as Mg(1)–K(1)–K(2)–Mg(2) in crystallographically non-equivalent sites along the three-fold symmetry axis.

There is a series of compounds named after that mineral, mostly synthetic crystals. In the general formula $A_2B_2(SO_4)_3$ there may be $A^+ = NH_4^+, K^+, Rb^+, Cs^+, Tl^+$ and $B^{2+} = Mg^{2+}, Ca^{2+}, Mn^{2+}, Fe^{2+}, Co^{2+}, Ni^{2+}, Zn^{2+}$ or Cd^{2+}. Up to now 29 out of the conceivable cation combinations are known [2–4]. Some of them are peculiar in showing improper phase transitions, the low temperature phase being ferroelectric [5–7]. The high temperature phase, however, is in any case isomorphous to the first mentioned langbeinite. Structure refinements have been reported for a number of these crystals [1–3, 8, 9, 11, 20].

Impurity elements can be incorporated into langbeinites, but those defects have only scarcely been investigated. Apart from UV studies, a few electron paramagnetic resonance (EPR) studies of langbeinites with $A = NH_4^+, Rb^+, Tl^+$ and $B = Cd^{2+}$ were undertaken using Mn^{2+} [12–16, 20], Cu^{2+} [10] and VO^{2+} [14] ions as paramagnetic dopants and focussing attention on phase transitions. Some other reported data appear to refer to ill defined crystals [17–19]. Therefore a systematic EPR study covering as many langbeinites as possible seems worthwhile regardless of the occurrence of phase transitions. Especially the S-state transition metal ions Mn^{2+} and Fe^{3+} are promising as structural probes since there is a wealth of experience on their EPR properties, in particular the structure dependence of their zero field splitting (ZFS) parameters as described by the so called superposition model (SPM).

The present work is concerned with the cubic high temperature phase of langbeinites doped with Mn^{2+}, while results obtained with Fe^{3+} will be reported in a subsequent paper. The objectives are to gather information on the possibility of Mn^{2+} incorporation and to find out by EPR the sites occupied and the structure of the defects. The above-mentioned Mn^{2+} EPR studies [13–16, 20] agree in assigning Mn^{2+} to a site with three-fold axial symmetry, probably substituting the B ion Cd^{2+}. Some problems, however, still need clarification, e.g. as to whether one or both of the non-equivalent sites are concerned and as to the sign of the second order ZFS parameter B_2^0, which shall be elucidated in the present work. It is intended to consider all langbeinites feasible, the B ion Mn^{2+} of course excepted for simple reasons. Also the B ion

[a] Deceased.

Reprint requests to Prof. M. Stockhausen, Institut für Physikalische Chemie der Universität, Schloßplatz 4, W-4400 Münster (Germany).

0932-0784 / 92 / 0700-0849 $ 01.30/0. – Please order a reprint rather than making your own copy.

Fe^{2+} is excluded as there is a risk of interferences with the paramagnetic host lattice.

Experimental

Preparation of Samples

Following the literature [13–16, 20] it was tried to prepare manganese doped langbeinites, using A_2SO_4 and $BSO_4 \cdot xH_2O$ and the corresponding manganese salt (p.a. from Merck) as educts. Crystals were grown either from the melt (Bridgman-Stockbarger [3, 21–23] and Tamman-Stöber method [23]), by slow evaporation from aqueous solution [24, 25] or fast evaporation [2, 4], in which case the product was subsequently tempered (1 d at about 600 K). In most cases single crystals of sufficient size and quality for EPR measurements could be obtained. If not, the materials could be used for the measurement of EPR powder spectra only.

Sometimes obviously $A_2B(SO_4)_2 \cdot (6 \cdots 7)H_2O$ double sulfates resulted. In order to avoid uncertainties in that respect, all products were analyzed or characterized by one or more of the following methods: Complexometric titration with EDTA against eriochrome black T, assessment of the EPR powder spectrum under the assumption that a divalent site with axial symmetry should be occupied as in the cases so far known [13–16, 20], test on water-free substance (when grown from aqueous solution), morphology, colour and homogeneity of the crystals.

For a selected system, namely NH_4–Cd langbeinite, the equilibrium of manganese incorporation was studied in more detail by changing the manganese mole fraction in the growth solution, x_{sol}, between $0.6 \cdot 10^{-3}$ and $170 \cdot 10^{-3}$. The manganese mole fraction in the langbeinite crystal was found to exceed x_{sol} by about 30 percent (correlation coefficient $r = 0.95$). This is strongly indicative of a substitutional incorporation of Mn in Cd sites.

The langbeinites obtained and measured are listed in Table 1. The Mn^{2+} mole fraction is $x_{Mn^{2+}} \leqq 0.01$ for all samples studied. Doped langbeinites with $A = K^+$ and $B = Co^{2+}$, Ni^{2+}, were obtained, too, by the Bridgman method. The definite composition of these water-free crystals (colour violet or yellow, respecsubstances are therefore omitted from Table 1 and shall not further be regarded.

Table 1. The Mn^{2+} doped langbeinites, preparation methods, properties and methods applied for analysis.

Langbeinite A	Langbeinite B	Preparation[a]	Quality[b]	Method of analysis[c]				
				1	2	3	4	5
Rb	Mg	1	S	–	+	–	–	+
Tl	Mg	4	P	–	+	–	–	–
NH_4	Mg	4	P	–	+	–	–	–
K	Mg	1	S	+	+	–	–	+
K	Zn	1	S	+	+	–	–	–
Rb	Cd	3	S	+	+	+	+	–
Tl	Cd	3	S	+	+	+	+	–
NH_4	Cd	3	S	+	+	–	+	–
K	Cd	1,2	S	+	+	–	–	(+)
Rb	Ca	1	P	–	+	–	–	–
K	Ca	1	P	–	+	–	–	–

[a] 1: Bridgman-Stockbarger, 2: Tamman-Stöber, 3: from solution, slow evaporation, 4: from solution, fast evaporation, tempered.

[b] S: Single crystal, P: powder (colourless or white, respectively).

[c] 1: Titration, 2: EPR powder spectrum, 3: crystal water, 4: morphology, 5: homogeneity.

EPR Spectroscopy and Treatment of Data

EPR measurements were carried out at X-band employing a Bruker spectrometer ESP 300, which for temperature dependent measurements was equipped with a closed-cycle system (low temperatures) or with a gas flux system (elevated temperatures). The B_0 field was measured with a Hall probe, and the microwave frequency was determined using picein as standard [26].

Powder spectra were taken from all the langbeinites given in Table 1. Provided that suitable single crystals were available, the angular variation of the EPR signals, viz. rotation diagrams, were measured in addition. Spectra were recorded at 2° intervals for that purpose. The rotation axis was chosen parallel to the (111) plane so that the $z \parallel \boldsymbol{B}_0$ direction is included in the rotation path, magnetic z denoting here the threefold symmetry axis ([111] space diagonal of the unit cell). The spectra were evaluated according to a spin-Hamiltonian $\mathcal{H} = \mathcal{H}_Z + \mathcal{H}_{ZFS} + \mathcal{H}_{HFS}$ with

$$\mathcal{H}_Z = \beta \boldsymbol{B}_0 g \boldsymbol{S}, \quad \mathcal{H}_{ZFS} = \sum_{n=2,\text{even}}^{2 \cdot \text{ent}S} \sum_{m=-n}^{n} B_n^m \mathcal{O}_n^m,$$

$$\mathcal{H}_{HFS} = \boldsymbol{S} A \boldsymbol{I},$$

i.e. using the spherical operator representation of the zero field splitting term $\mathcal{H}_{ZFS}$. The parameters of the spin-Hamiltonian were derived by fitting calculated peak positions to the observed ones and checking the

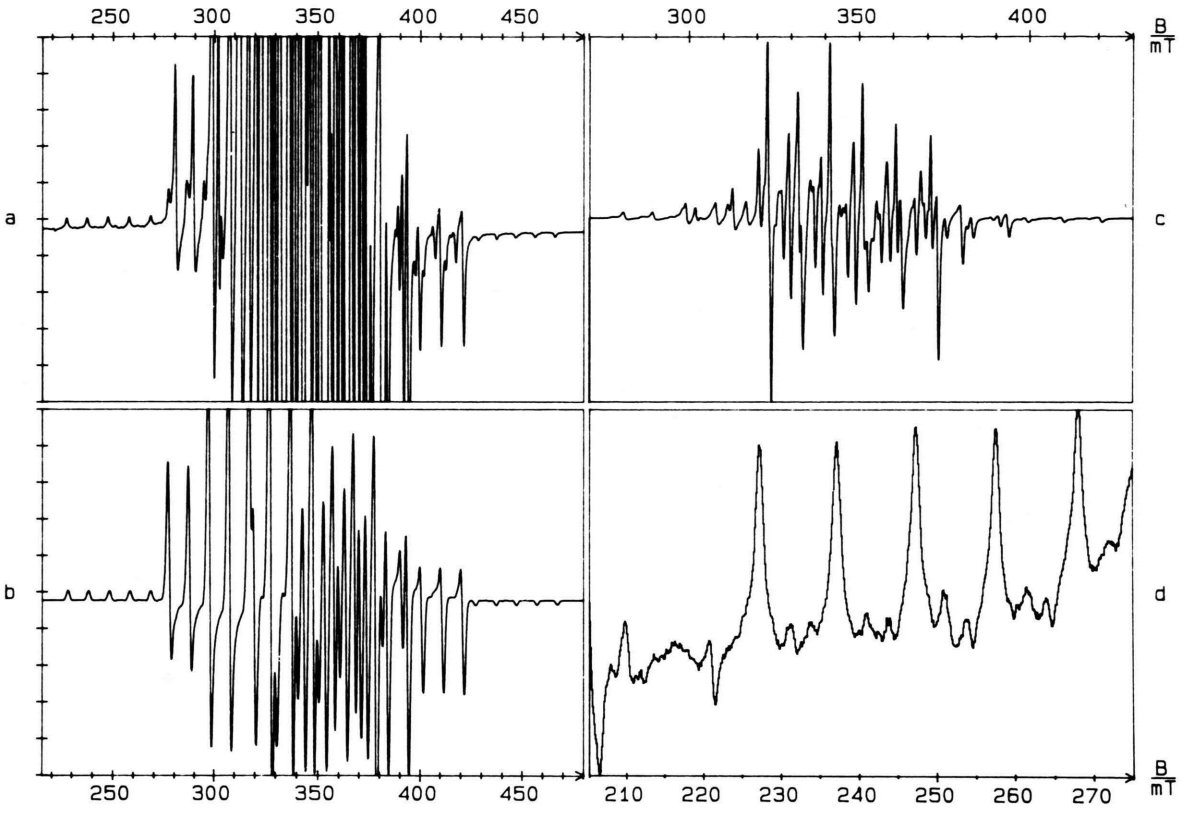

Fig. 1. Powder spectrum of Mn^{2+} in K–Mg langbeinite at room temperature. Left, overview: (a) Experimental, (b) simulation. Right, details: (c) Central region with reduced amplification, (d) low field region with enhanced amplification.

results by simulation of the powder spectra (introducing linewidths as external parameters) or rotation diagrams. The parameters A_i for a certain direction i were directly obtained from the hyperfine sextets as averaged values from all transitions assigned to the respective direction. Only the sextet centers were then taken into account by the fitting procedure. Due to the relatively small zero field splitting observed with the present substances there remains an uncertainty in determining the centers of the hyperfine sextets. This allows to reckon with an isotropic g-factor $g = 2.0023$ in all cases. Consequently B_2^0 is the main fitting parameter, while further ZFS parameters (particularly B_4^0) were considered in the fitting procedure but were found to be less accurately determinable. They will therefore not be reported in the following.

Various software was available for the data evaluation. The ZFS parameters were fitted to the rotation diagrams using a program by Remme [27]. Powder spectra were simulated by a program newly written for that purpose, while for the simulation of rotation diagrams a program by Prissok was employed [26].

Results and Discussion

Common Features

The powder spectra of all samples are readily assignable to a Mn^{2+} center C(1) of axial symmetry, which is not unexpected and is also in accord with previous EPR results [13–16, 20]. A typical example is represented in Figure 1. Except for the Tl–Mg langbeinite there is no indication of a second defect. However, the rotation diagrams reveal a second center C(2) of weak intensity, exhibiting larger ZFS but the same direction of magnetic axes as C(1). Figure 2 shows a rotation diagram together with its simulation (the latter restricted to the centers of the HFS sextets) as example.

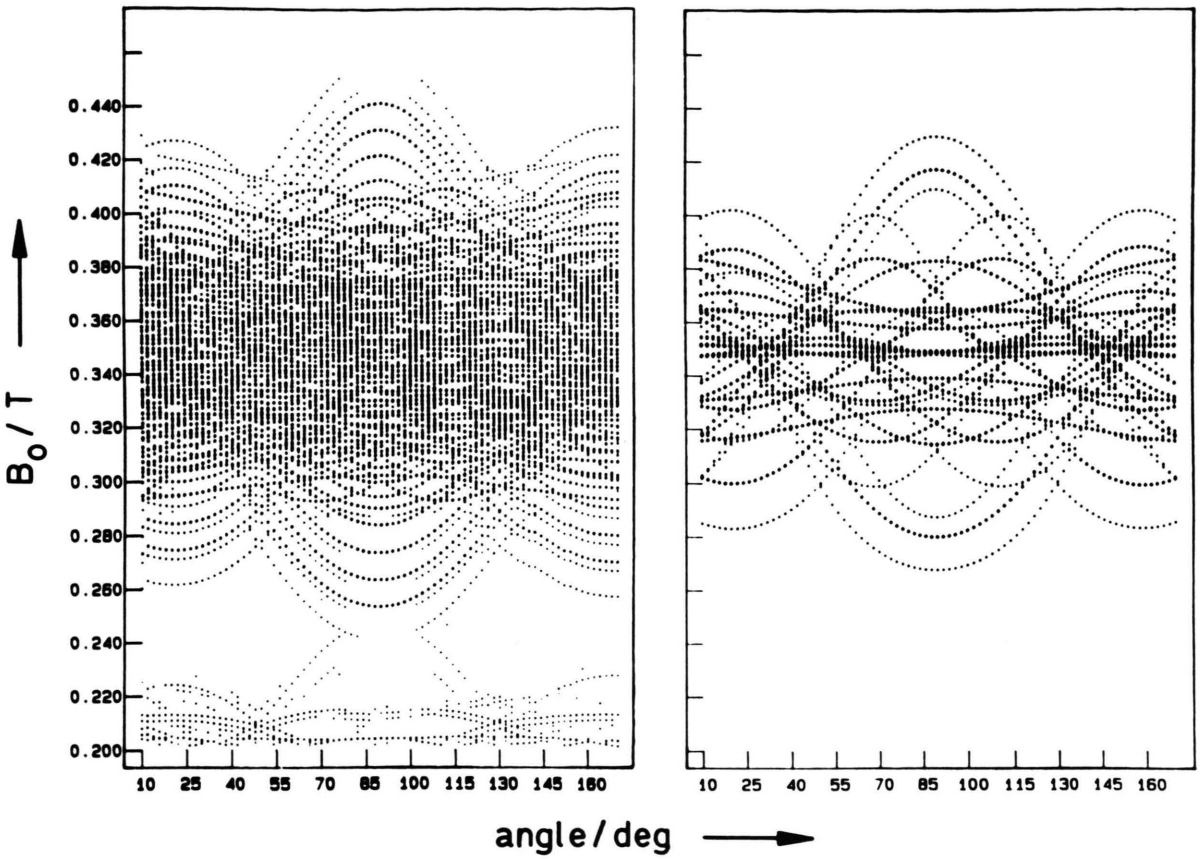

Fig. 2. Rotation diagram of the single crystal spectrum of Mn^{2+} in NH_4-Cd langbeinite (9.77 GHz). *Left:* Experimental. *Right:* Simulation (centers of hyperfine sextets only). The rotation angle of 90° corresponds to $z \parallel \boldsymbol{B}_0$.

Zero Field Splitting

The ZFS parameters B_2^0 for both centers C(1) and C(2) are summarized in Table 2. For C(1), their sign could be determined directly in some cases (i.e. for Rb–Mg, NH_4–Cd and Tl–Cd langbeinite) from temperature dependent measurements over a range where phase transitions do not occur (that is between 50 to 300 K for Rb–Mg, 115 to 300 K for NH_4–Cd and 150 to 300 K for Tl–Cd langbeinite). The ratio of the low field sextet intensity in relation to that of the high field sextet is >1 and decreases with increasing temperature, from which the sign of B_2^0 follows. According to the obvious similarity of the Mn^{2+} centers in all langbeinites a negative sign of B_2^0 can reasonably be assumed also for the other C(1) cases. An additional argument in favour of the negative sign is provided by the HFS parameters considered in the subsequent section.

A closer inspection of the absolute values of B_2^0 reveals correlations with the ionic radii $r_{A,B}$ of both A and B type ions. This is particularly the case with respect to the B ions, where $|B_2^0|$ appears to vary with r_B in a contravariant manner. The A ions, on the other hand, induce an opposite though less clear tendency. A satisfactory correlation is found by regarding the ratio of ionic radii of B and A ions of the host lattice, $Q = r_B/r_A$. Using for Q the radii given in Table 3, one obtains for C(1) and C(2) the correlations depicted in Figure 3. Disregarding the C(1) point of Tl–Mg langbeinite, the regression lines as drawn in the figure indicate that differences between C(1) and C(2) become negligible for Q values in the $Q \approx 0.45 \ldots 0.5$ range.

The systematic dependence of B_2^0 on the ionic radii of B as well as A ions can be accounted for by distortions of the neighbourhood of the probe ion if this is supposed to occupy a B site. Depending on whether

Table 2. ZFS parameters of Mn^{2+} doped langbeinites. Measured ZFS parameter B_2^0, parameters D_z and $\bar{B}_2$ obtained by a SPM analysis, and intensity ratio $I(1)/I(2)$ of spectra assigned to centers C(1) and C(2).

Langbeinite A	B	T/K	Center[a]	B_2^0/GHz	D_z ±0.009	$\bar{B}_2$/GHz	$I(1)/I(2)$
Rb	Mg	RT	1,2	−0.259(9)	–	–	–
Tl	Mg	RT	1	−0.204(4)	–	–	≈ 5
			2	∓0.260(9)	–	–	
NH_4	Mg	RT	1	−0.242(2)	–	–	–
K	Mg	RT	1	−0.221(6)	−0.182	+1.21	≈ 30
			2	∓0.230(9)	−0.508	±0.46	
K	Zn	RT	1	−0.209(2)	−0.240	+0.87	≈ 35
			2	∓0.230(9)	−0.774	±0.31	
Rb	Cd	RT	1	−0.177(2)	–	–	≈220
			2	∓0.234(9)	–	–	
Tl	Cd	RT	1	−0.153(5)	–	–	≈250
			2	∓0.210(9)	–	–	
NH_4	Cd	RT	1	−0.162(2)	−0.145	+1.12	≈500
			2	∓0.218(8)	−0.492	±0.44	
K	Cd	423	1	−0.137(5)	−0.231	+0.59	–
			2	–	−0.645	–	
Rb	Ca	RT	1	−0.150(3)	–	–	–
K	Ca	486	1	−0.102(5)	−0.121	+0.84	–
			2	–	−0.395	–	

[a] Centers marked "1" and "2" refer to the more or less spacious site, respectively.

Table 3. Ionic radii r [28, 29].

Ion	r/pm	Ion	r/pm
Mg^{2+}	72.0	K^+	138
Zn^{2+}	74.0	NH_4^+	143
Cd^{2+}	95.0	Tl^+	150
Ca^2	100.0	Rb^+	152
		Cs^+	167
Mn^{2+}	83.0		

the host ion B is larger or smaller than the probe ion Mn, the ligand shell may be expanded or contracted, respectively, without lowering the symmetry. The local structural relaxation may involve the A type cation via the sulfate groups separating the A and B sites.

Further structural information may possibly be gained by application of the superposition model (SPM) of ZFS parameters [30] which is well established for the Mn^{2+} ion [31]. This model postulates independent ligand contributions to the ZFS parameters B_n^m from the nearest neighbours only, according to

$$B_n^m = \sum_{i=1}^{N} K_n^m(\theta_i, \phi_i)\, \bar{B}_n(i, R_i),$$

where i denotes the ligand and θ_i, ϕ_i, R_i its position relative to the probe ion with respect to the principal axes (x, y, z) of the ZFS tensor. The K_n^m are spherical harmonics of order n. The radial factor $\bar{B}_n$ was empirically found to depend on R_i approximately as a power law

$$\bar{B}_n(i, R_i) = \bar{B}_n(i, R_0)\left(\frac{R_0}{R_i}\right)^{t_n}.$$

Here R_0 is a typical value for bond lengths of the probe ion. For the present case the ligands to be regarded are six oxygens. For those ligands $t_2 \approx 7$ is found empirically. The second order ZFS parameter under consideration (where $m = 0$) can thus be written as a product

$$B_2^0 = \bar{B}_2 \cdot D_z$$

with the intrinsic ZFS parameter $\bar{B}_2 = \bar{B}_2(i = \mathrm{O}, R_0)$ and the so called distortion function, referring here to the magnetic z direction,

$$D_z(\theta_i, R_i) = \sum_{i=1}^{6} \frac{1}{2}(3\cos^2\theta_i - 1)\left(\frac{R_0}{R_i}\right)^7,$$

which can be calculated from structural data. Provided the model be valid, $\bar{B}_2$ is characteristic of the host crystal, and with $\bar{B}_2 > 0$ one expects $B_2^0 \sim D_z$, $\operatorname{sgn} B_2^0 = \operatorname{sgn} D_z$.

Structure refinements are available for (undoped) K–Mg, K–Zn, NH_4–Cd, K–Cd and K–Ca langbeinites [1, 3, 9, 11, 20]. From these structural data the distortion function D_z was calculated (with $R_0 = 220$ pm) for both B sites. It turned out that in any case $\operatorname{sgn} D_z = -1$ and that the more spacious site is characterized by smaller absolute values $|D_z|$. There is an obvious parallelism with the distortion interpretation of B_2^0 (Fig. 3) which allows to assign C(1) to the more spacious B site and C(2) to the less spacious one. That inference is supported by calculations on NH_4–Cd langbeinite [20] which yield $B_2^0 = -0.157$ and -0.200 GHz for the more and the less spacious site, respectively, which is in good agreement with the values measured in this work. The D_z values are given in Table 2 in accord with the proposed assignment. In addition, $\bar{B}_2 = B_2^0/D_z$ is listet in that table.

There is no hint from the SPM analysis as to a correlation of the SPM parameters with the ratio of ionic radii Q. Thus the conclusion appears that the correlation shown in Fig. 3 is not at all ascribable to the undisturbed langbeinite structure but is an effect of

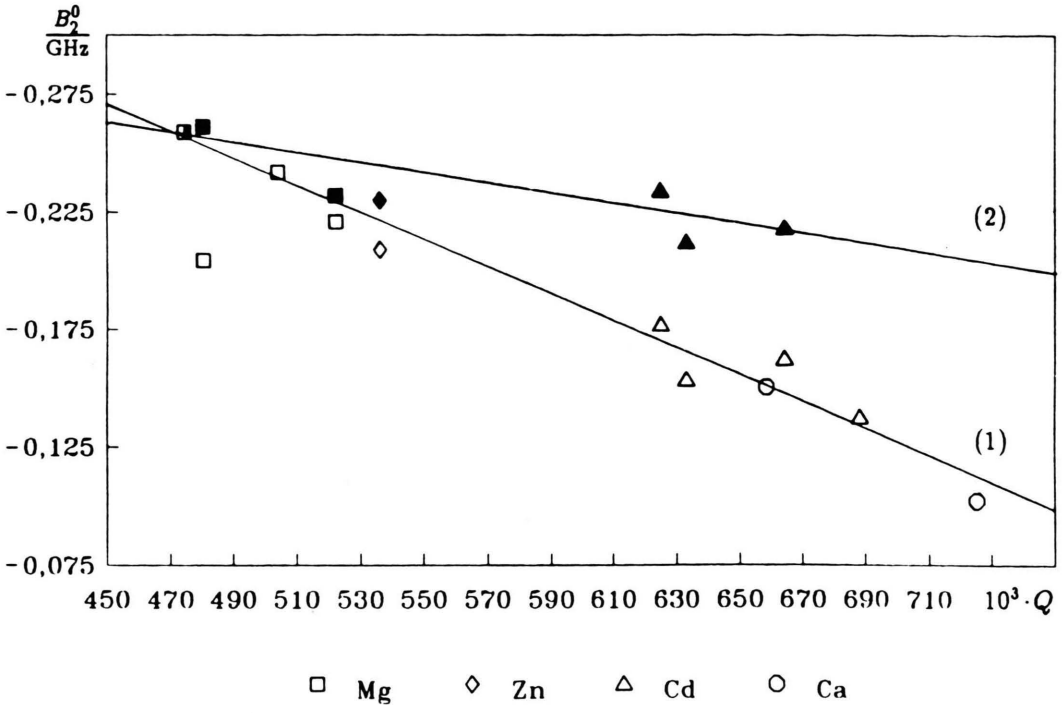

Fig. 3. ZFS parameter B_2^0 against ratio of ionic radii, $Q = r_B/r_A$, for centers C(1) and C(2) (open and full symbols, respectively).

Table 4. HFS parameters $A_\parallel$ and $A_\perp$ of the Mn^{2+} doped langbeinites, for center C(1).

Langbeinite A	Langbeinite B	T / K	$-A_\parallel$ / $10^{-4}\,cm^{-1}$	$-A_\perp$ / $10^{-4}\,cm^{-1}$	$\lvert A_\parallel\rvert - \lvert A_\perp\rvert$ / $10^{-4}\,cm^{-1}$	$A_\parallel$ (low)[a] / $A_\parallel$ (high)
Rb	Mg	RT	93.4(10)	91.9(10)	1.5(20)	1.10(2)
Tl	Mg	RT	93.8(15)	92.9(15)	0.9(30)	1.06(2)
NH_4	Mg	RT	93.1(15)	86.7(15)	6.4(30)	1.11(2)
K	Mg	RT	89.4(15)	89.0(15)	0.4(30)	1.12(2)
K	Zn	RT	91.3(15)	88.2(15)	3.1(30)	1.10(2)
Rb	Cd	RT	92.7(15)	85.6(15)	7.1(30)	1.06(2)
Tl	Cd	RT	88.8(15)	86.5(15)	2.3(30)	1.06(2)
NH_4	Cd	RT	93.1(25)	88.1(15)	5.0(30)	1.10(2)
K	Cd	423	94.2(15)	–	–	1.02(2)
Rb	Ca	RT	88.8(15)	83.7(15)	5.1(30)	1.08(2)
K	Ca	486	90.3(20)	–	–	≈1

[a] $A_\parallel$ from lowest and highest field HFS sextet, respectively.

local structural relaxation in the vicinity of the probe ion.

Lastly the intensity ratio of the C(1) and C(2) spectra, which is also given in Table 2, should be mentioned. It increases with increasing ratio Q. This may be accounted for by a preferential occupation of the very B site which allows for the more pronounced local relaxation.

Hyperfine Splitting

The HFS parameters of C(1) are summarized in Table 4. Since $|A_\parallel| > |A_\perp|$ in all cases, a trigonal distortion of the ligand sphere around the probe ion, stretched along the z-axis, is likely [32]. Some of the absolute $|A_i|$ values are slightly higher than usually found for six-fold oxygen coordination of Mn^{2+}

(ranging between $80 \ldots 88 \cdot 10^{-4}\,cm^{-1}$ [33]) but the deviation is still small. The HFS expected for nine-fold coordination as for an A site would be in the same order, so the A_i values cannot be considered as decisive in any way. Other than B_2^0, $A_{\parallel}$ shows not any discernible correlation with the ratio Q of ionic radii, while at least $A_{\perp}$ seems to be weakly positively correlated.

In the last column of Table 4 the ratio of $A_{\parallel}$ as measured for the low and high field sextet is given. Since the ratio is > 1 and, as far as known from numerous experiments, sgn $A_{\parallel} = -1$ for Mn^{2+} [34], this corroborates the conclusion on the negative sign of B_2^0 already drawn above.

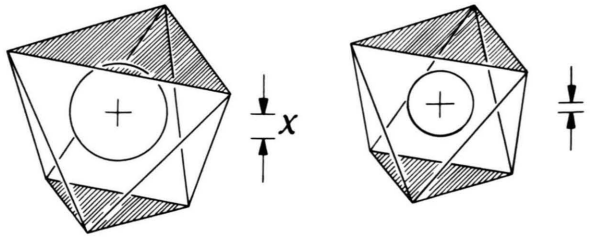

Fig. 4. Schematic representation of distorted octahedral ligand arrangement around the B site when occupied by a host B^{2+} ion (left) or by the Mn^{2+} probe ion after relaxation (right). The distortion parameter X is indicated; the parameter Δ relates qualitatively to the difference of the hatched triangle areas.

Relaxation Model

The observations discussed so far can at least qualitatively be explained by some assumptions on the local relaxation around B sites occupied by Mn^{2+} ions. As starting point we refer to the structure refinement of K–Ca langbeinite reported by Speer and Salje [3]. They describe the deviation of the oxygen ligands around Ca^{2+} from O_h symmetry by a number of parameters. Referring to planes perpendicular to the three-fold symmetry axis, three oxygens are arranged in a triangle "above" and the other three oxygens in a triangle "below" the central ion. The parameter Δ describes the relative difference of the areas of both triangles, and ϕ is the deviation from their regular twist angle (60°). By X the shift of the cation from its central position towards one (the larger) triangle is denoted, and δ is the mean distance between cation and triangle planes. The left hand part of Fig. 4 illustrates the situation in the undoped langbeinite, the circle indicating the central cation (e.g. Ca). Now let this be substituted by a smaller cation such as Mn. The surrounding oxygens can then relax towards the center of the octahedron as sketched on the right hand side of Figure 4. Possibly the surrounding oxygens may contact the central ion. Qualitatively it seems plausible that such a relaxation will result in decreased parameters Δ, X, and δ, so that the oxygens more closely approach O_h symmetry. If this should be the case, alterations of the ZFS parameters discussed above should occur as observed, and the different behaviour of C(1) and C(2) would be understandable, too.

Concluding Remark

The present study has cleared up the uncertainty concerning the sign of the ZFS parameter B_2^0 related to the main center of Mn^{2+} doped langbeinites, and it has shown that the two non-equivalent B sites can in fact both be occupied by the divalent impurity ion. Although the overall behaviour of the 11 doped systems which we have investigated is rather similar in exhibiting only these two kinds of substitutional centers, there are systematic tendencies depending on the ionic radii which indicate a more-or-less considerable relaxation. From this it appears understandable in retrospect that the superposition model, which relies upon well defined, undisturbed ligand positions does not work satisfactorily for these examples.

Acknowledgement

Support by the Deutsche Forschungsgemeinschaft and by the Fonds der Chemischen Industrie is gratefully acknowledged.

[1] A. Zemann and J. Zemann, Acta Cryst. **10,** 409 (1957).
[2] G. Gattow and J. Zemann, Z. Anorg. Allg. Chem. **293,** 233 (1958).
[3] D. Speer and E. Salje, Phys. Chem. Minerals **13,** 17 (1986).
[4] M. Kharizi and M. O. Steinitz, Solid State Comm. **66,** 375 (1988).
[5] F. Jona and R. Pepinsky, Phys. Rev. **103,** 1126 (1956).
[6] N. Yamada, J. Phys. Soc. Japan **46,** 561 (1979).
[7] M. Glogarová and J. Fousek, phys. stat. sol. (a) **15,** 579 (1973).
[8] N. Yamada, M. Maeda, and H. Adachi, J. Phys. Soc. Japan **50,** 907 (1981).
[9] M. J. L. Percival, W. W. Schmahl, and E. Salje, Phys. Chem. Minerals **16,** 569 (1989).
[10] V. C. Mouli and G. S. Sastry, J. Mol. Struct. **96,** 163 (1982).
[11] S. C. Abrahams, F. Lissalde, and J. L. Bernstein, J. Chem. Phys. **68,** 1926 (1978).
[12] I. Tatsuzaki, J. Phys. Soc. Japan **17,** 1312 (1962).
[13] S. K. Misra and S. Z. Korczak, J. Phys. C **19,** 4353 (1986).
[14] D. S. Babu, G. S. Sastry, M. D. Sastry, and A. G. I. Dalvi, J. Phys. C **17,** 4245 (1984).
[15] S. K. Misra and S. Z. Korczak, Solid State Comm. **61,** 665 (1987).
[16] S. K. Misra and S. Z. Korczak, J. Phys. C **20,** 4485 (1987).
[17] B. V. R. Chowdari, J. Phys. Chem. Solids **30,** 2747 (1969).
[18] B. V. R. Chowdari, J. Phys. Chem. Solids **31,** 1408 (1970).
[19] G. C. Upreti, J. Phys. Chem. Solids **35,** 461 (1974).
[20] Hok Nam Ng and C. Calvo, Can. J. Chem. **53,** 1449 (1975).
[21] J. Liebertz and P. Quadflieg, J. Cryst. Growth **6,** 109 (1969).
[22] K. Nassau and J. W. Shiever, J. Cryst. Growth **42,** 588 (1977).
[23] K.-T. Wilke and J. Bohm, Kristallzüchtung, Deutsch, Thun 1988.
[24] B. Březina and A. Fousková, Kristall und Technik **13,** 623 (1978).
[25] B. Březina and M. Havránková, J. Cryst. Growth **21,** 77 (1974).
[26] F. Prissok, Thesis Münster 1989.
[27] S. Remme, Thesis Münster 1985.
[28] R. D. Shannon, Acta Cryst. **A 32,** 751 (1976).
[29] R. C. Weast (Ed.), CRC Handbook of Chemistry and Physics, 64th ed., CRC Press, Boca Raton 1983.
[30] D. J. Newman and W. Urban, Adv. Phys. **24,** 793 (1975).
[31] R. Büscher, Thesis Münster 1985.
[32] G. Lehmann, J. Phys. Chem. Solids **41,** 919 (1980).
[33] E. Šimánek and K. A. Müller, J. Phys. Chem. Solids **31,** 1027 (1970).
[34] A. D. Rae, J. Chem. Phys. **50,** 2672 (1969).